Low valent Al(II)–Al(II) catalysts as highly active ϵ-caprolactone polymerization catalysts: indication of metal cooperativity through DFT studies

Olga Kazarina, Christophe Gourlaouen, Lydia Karmazin, Alexander Morozov, Igor Fedushkin, Samuel Dagorne

Low Valent Al(II)–Al(II) Catalysts as Highly Active ε-caprolactone polymerization catalysts: indication for metal cooperativity through DFT studies

Olga V. Kazarina,[a,b] Christophe Gourlaouen,[a] Lydia Karmazin,[c] Alexander G. Morozov,[b] Igor L. Fedushkin,[b*] Samuel Dagorne[a*]

[a]*Institut de Chimie (UMR CNRS 7177)- Université de Strasbourg; 4, rue Blaise Pascal, 67000 Strasbourg, France, Email: dagorne@unistra.fr*

[b]*G.A. Razuvaev Institute of Organometallic Chemistry of Russian Academy of Sciences, Tropinina str. 49, 603950 Nizhny Novgorod, Russian Federation, Email: igorfed@iomc.ras.ru*

[c] *Service de Radiocristallographie, CNRS-Université de Strasbourg, UMR 7177, 1 Rue Blaise Pascal, F-67000 Strasbourg, France*

Abstract. The present study first describes the reactivity of low valent Al(II) and Ga(II) complexes of the type (dpp-bian)M–M(dpp-bian) (**1**, M = Al; **2**, Ga; dpp-bian^{2-} = 1,2-*bis*-(2,6-iPr_2-C_6H_3)-acenaphthenequinonediamido) with cyclic esters/carbonates such as ε-caprolactone (CL) and trimethylene carbonate (TMC). CL and TMC both readily coordinates to the Al(II) species **1** to form the corresponding *bis*-adducts (dpp-bian)Al(L)–(L)Al(dpp-bian) (**3**, L = CL; **4**, L = TMC), which were structurally characterized confirming that the Al(II)–Al(II) dimetallic backbone retains its integrity in the presence such cyclic polar substrates. In contrast, the less Lewis acidic Ga(II) analogue **2** shows no reaction in the presence of stoichiometric amount of CL and TMC at room temperature. In combination with BnOH, the dinuclear Al(II) species **1** revealed to be an extremely active Al(II) initiator for the controlled ROP of CL at room temperature, outperforming all its Al(III) congeners thus far reported. Detailed DFT studies on the ROP mechanism are consistent with a process occurring thanks to metallic cooperativity between the two Al(II) proximal (since directly bonded) metal centers in **1**, which undoubtedly favors the ROP process through bimetallic activation and thus rationalize the unusually high CL ROP activity at room temperature.

Introduction

Poly(ε-caprolactone) (PCL) and poly(trimethylene carbonate) (PTMC) are biodegradable and biocompatible polyesters/polycarbonates of current interest for a growing number of applications, most notably in biomedicine.[1,2] In particular, PCL is an important material due to its miscibility with various other polymers and slow biodegradation rate, making it a biomaterial of choice for long-term implantable devices. PTMC is typically for biomedical applications as non-semi-crystalline and non-brittle biomaterial. The controlled production of PCL and PTMC is most conveniently achieved *via* ring-opening polymerization of ε-caprolactone (CL) and trimethylenecarbonate (TMC), respectively, using metal-based complexes, allowing access to well-defined and chain-length-controlled PCL material.[1,2,3] Over the past twenty years, the design and synthesis of various metal-based catalysts (essentially with oxophilic and Lewis acidic metal centers) have been intensively studied to achieve high activity and control in the ROP of CL and, to a lesser extent, of TMC.[3,4] In that regard, bimetallic metal ROP catalysts have recently attracted attention for improved ROP performance: *i.e.* the presence of two proximal metal centers within the same molecule may promote cooperative effects for enhanced ROP activity. Thus far, strategies to access well-defined bimetallic ROP catalysts have primarily relied on the use of ligand platforms containing two N-/O-based chelating entities, one per metal center, with each metal chelate linked to one another *via* a spacer imposing proximity between the metal centers for bimetallic cooperation. Recent and representative of such dinuclear ROP catalysts are depicted in Figure 1 (**A**-**D**).[5] There are also a number of dinuclear metal ROP catalysts supported by ligands bridging two metal centers (such as alkoxides/halide bridges of the type M–(μ-X)–M (X = halide, OR) for which the beneficial role of dinuclearity on ROP performance was clearly demonstrated, most notably in the case of In(III) derivatives (**E**-**G**, Figure 2).[6]

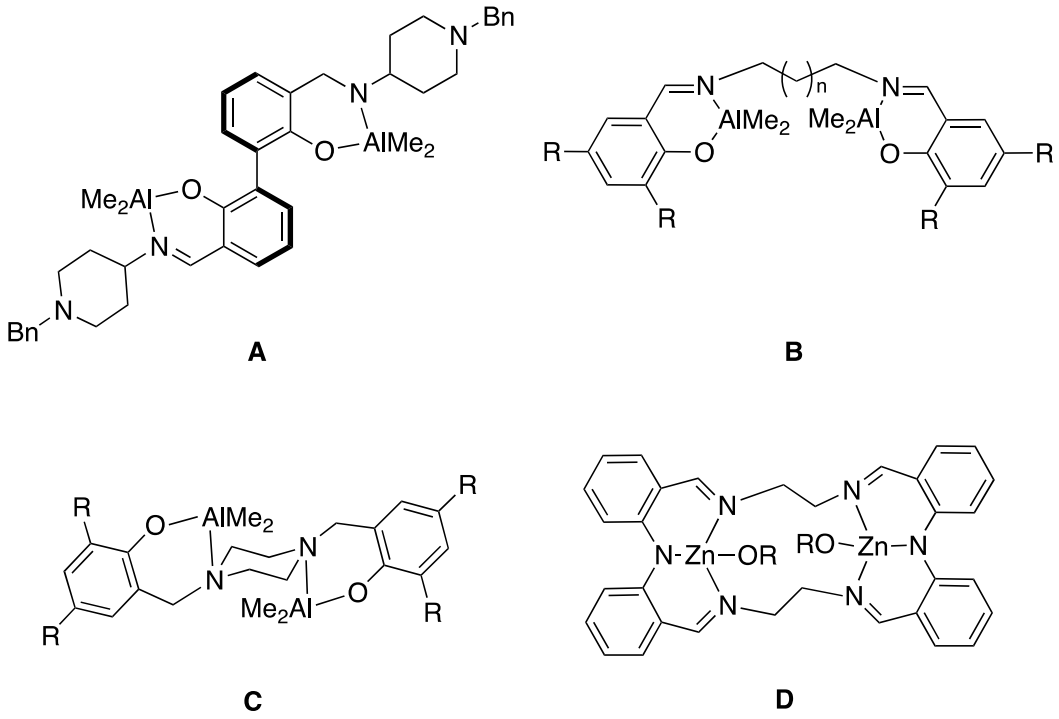

Figure 1. Representative dinuclear ROP catalysts supported *bis*-chelating ligand platforms linked by a spacer.

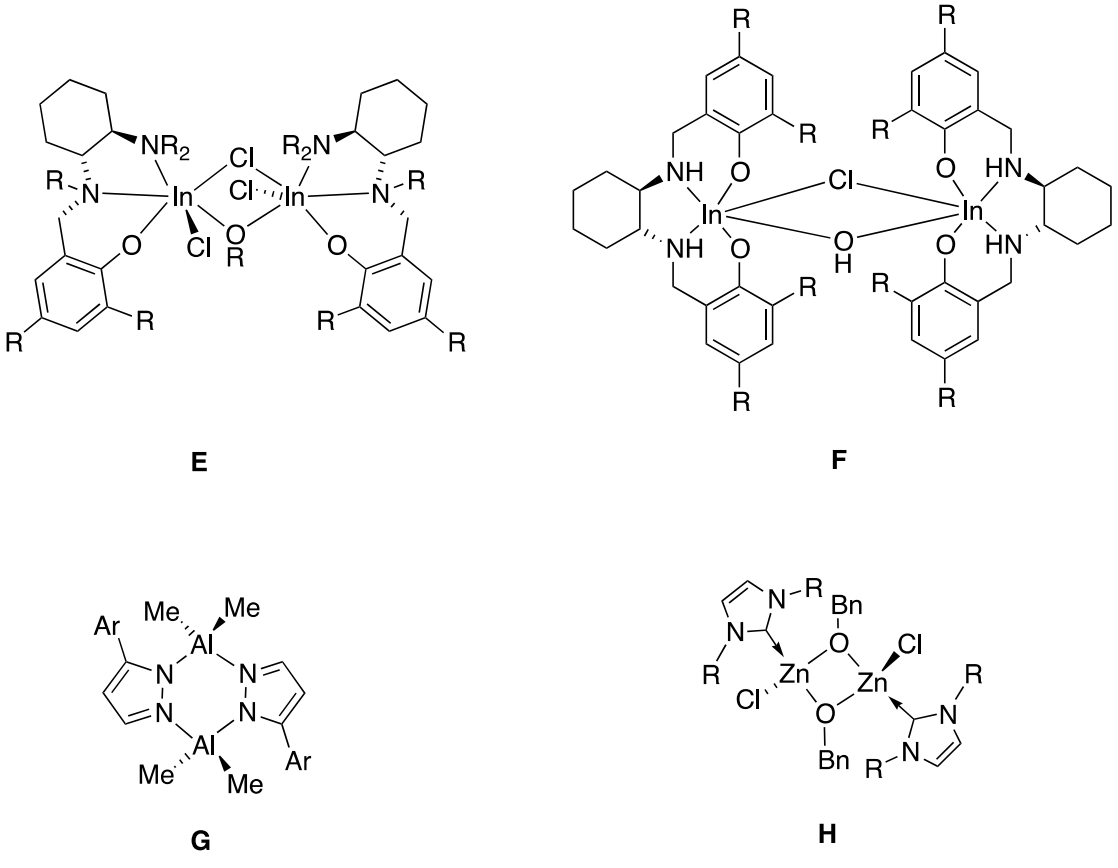

Figure 2. Representative dinuclear ROP catalysts with bridging ligands connecting the two co-operative metal centers

Bimetallic Al(II) and Ga(II) complexes supported by 1,2-*bis*-(2,6-iPr$_2$-C$_6$H$_3$)-iminoacenaphthene (= dpp-bian) of the type (dpp-bian)M–M(dpp-bian) (**1** and **2**, Figure 3), thus containing two covalently bonded M(II) centers, remain rare examples of stable and robust group 13 metal M(II) compounds, and their ability to activate various organic substrates for unusual reactivity (frequently redox-related) has been demonstrated over the past few years.[7] Despite the lower Lewis acidity of M(II) *vs.* M(III) species (M = Al, Ga), the presence of a covalent M–M bond and thus of two proximal M(II) centers in species **1** and **2** is of particular interest within the context of ROP catalysis since potential co-operativity between the two M(II) centers may be expected. Also, to our knowledge, low valent group 13 metal species have not yet been exploited as cyclic esters/carbonates ROP catalysts, contrasting with the historical importance and numerous reports on group 13 M(III)-mediated ROP catalysis.[6a,8]

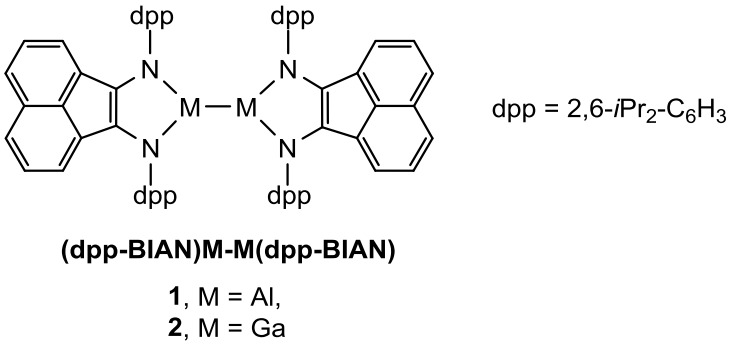

Figure 3. Dinuclear Al(II) and Ga(II) species **1** and **2** used as ROP catalysts in the present study

We herein report on the reactivity of Al(II) and Ga(II) species **1** and **2** with CL and TMC, and their use in ROP catalysis. In the case of Al(II) species **1**, found to be highly active in the ROP of CL, the ROP mechanism was thoroughly investigated by DFT studies, strongly hinting at a cooperative role between the two Al(II) centers.

Results - Discussion

Reactivity of dimetallic M(II) species 1 and 2 with CL and TMC: adducts characterization. Highly Lewis acidic three-/four-coordinate Al(III) and Ga(III) centers are well-known to readily activate/coordinate cyclic esters/carbonates such as CL and TMC, but the ability of less Lewis acidic M(II) analogues for similar activation is not known. Thus, compounds **1** and **2** were thus first probed for adduct formation with CL and TMC. The dialane **1** immediately reacts upon addition of two equivalent of TMC or CL (toluene, room temperature) leading to a color change from deep blue-violet to deep green. As monitored by ^{1}H NMR, the corresponding *bis*-adducts [(dpp-bian)Al(L)–(L)Al(dpp-bian)] (**3**, L = TMC; **4**, L = CL; Scheme 1) quantitatively formed and were isolated in high yields as deep green crystals. In contrast, under identical reaction conditions (toluene, room temperature), no reaction was observed between the Ga(II) analogue **2** and either TMC or CL, which reflects the lower Lewis acidity of Ga(II) *vs.* Al(II) centers and shows that three-coordinate Ga(II) centers in the (dpp-bian)M–M(dpp-bian) array may not be Lewis acidic enough for coordination of cyclic polar substrates.

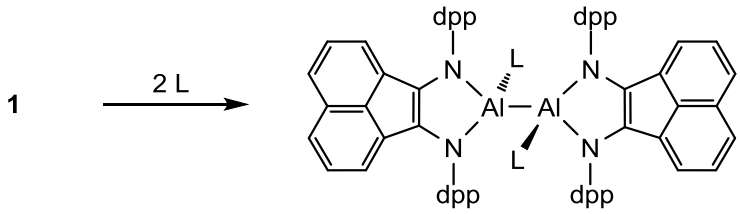

3, L = TMC
4, L = CL

Scheme 1. Formation of Al(II)–TMC and Al(II)–CL adducts **3** and **4**

The molecular structures of the Al(II)-L adducts **3** and **4** were unambiguously established by X-ray diffraction crystallographic analysis (for a summary of crystallographic data, see Table S1, ESI). To our knowledge, compound **3** is the first structurally authenticated metal–TMC adduct to be characterized. As depicted in Figure 4, the Al(II)-TMC adduct **3**, which crystallizes as a C_s-symmetric structure, thus evidences the effective coordination of a TMC monomer to each Al(II) center of the (dpp-bian)Al–Al(dpp-bian) backbone, with each TMC moiety being on opposite sides relative to the (dpp-bian)Al–Al(dpp-bian) backbone. Upon TMC coordination, both four-coordinate Al centers in **3** are only slightly pyramidalized to adopt a geometry best described as distorted trigonal monopyramidal. Importantly, all bonding/geometrical parameters in **3** agree with the Al(II) oxidation state with the diamido nature of each bian ligand being retained. In particular, the C(1)-C(2) bond length in **3** [1.376(3)] is nearly identical to that in base-free starting compound **1** [1.367(2) Å] while the Al-N(1) and Al-Al bond distances (1.876(2) and 2.585(1) Å, respectively) are slightly elongated relative to those in **1** (1.818 and 2.522 Å, respectively). The Al–O_{TMC} bond lengths in **3** (1.948(2) Å) are similar to the Al–O_{CL} bond lengths in **4** (1.940(5) Å average, *vide infra*).

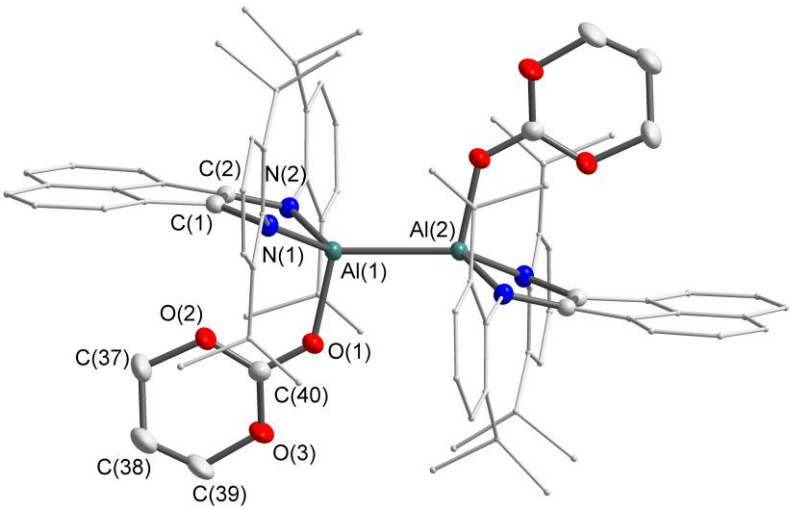

Figure 4. Molecular structure of the dinuclear Al(II)–TMC adduct **3**. Thermal ellipsoids are at 50% probability. Hydrogen atoms are omitted. Selected bond lengths (Å) and angles (°): Al(1)–Al(2) 2.5850(13), C(1)–C(2) 1.376(3), C(1)–N(1) 1.402(3), C(2)–N(2) 1.401(3), Al(1)–N(1) 1.876(2), Al(1)–N(2) 1.8762(19), Al(1)–O(1) 1.9484(16), O(1)–C(40) 1.239(40), Al(1)–O(1)–C(40) 130.54(16), N(1)–Al(1)–N(2) 91.29(8), O(1)–Al(1)–Al(2) 103.34(6).

Despite the poor quality of crystallographic data for the Al-CL adduct **4** (Table S1, Figure S6, ESI), atom connectivity and associated geometrical/bonding parameters could unambiguously be established for **4**, confirming its *bis*-adduct nature and its structural similarity to **3**. In line with a less Lewis acidic Al(II) *vs.* Al(III) center, the Al–O_{CL} bond lengths in **4** (1.940(5) Å average) is significantly longer than those in known Al(III)–CL adducts (1.852(6) Å average).[9]

ROP of CL catalyzed by species 1 and 2. The Al(II) and Ga(II) compounds **1** and **2** were tested as ROP catalysts for CL polymerization in the presence/absence of an alcohol source such as BnOH. The ROP results are compiled in Tables 1 and 2. All runs were performed at room temperature, showing species **1** and **2** initiate the ROP of CL under mild conditions. In the absence of BnOH, the ROP of CL mediated by **1** or **2** occurs with moderate activity and control, with the production of broadly disperse PCL exhibiting much higher M_n values than expected (entries 1 and 2, Table 1). The higher ROP activity of more Lewis acidic **1** (*vs.* **2**) along with the ill-defined ROP process strongly suggest a Lewis-acid-mediated ROP mechanism with the monomer itself acting as nucleophile. ^{1}H NMR monitoring of a 28/1 CL/**1** mixture (CD_2Cl_2, room temperature) led to the quantitative conversion of CL to PCL over the course of 3h along with the clean formation of adduct **4** (Figure S7, ESI).

Table 1. Room temperature ROP of ε-caprolactone catalyzed by compounds **1-2**[a].

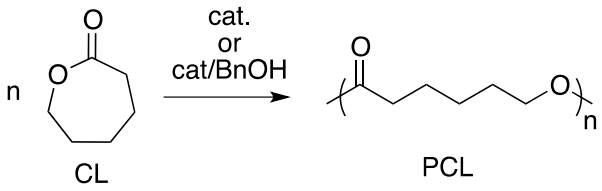

Entry	Cat.	CL (equiv)[b]	BnOH[b]	Time (h)[c]	Conv (%)[d]	$M_{n,\,theor}$[e]	$M_{n,\,exp}$[f]	$Đ$[g]	TOF (h^{-1})
1	**1**[h]	100	-	24	91	10400	30200	2.28	3.8
2	**2**[h]	100	-	24	57	6400	71300	1.22	2.4
3	**1**[h]	100	1	0.25	100	11400	10800	1.24	400
4	**2**[h]	100	1	24	100	11400	11900	1.67	4.2
5	**1**[h]	1000	10	0.25	93	10600	9900	1.06	3720

[a]Polymerization conditions: $[CL]_0$ = 1 M, room temperature. [b]Amount in equiv versus Al initiator. [c]Reaction time. [d]Monomer conversion. [e]Calculated using $M_{n,theor}$ = [ε-caprolactone]$_0$/[BnOH or catalyst]$_0$ × $M_{\varepsilon\text{-caprolactone}}$ × conversion. [f]Measured by GPC in THF (30 ˚C) using PS standards and corrected by applying the appropriate correcting factor (0.56). [g]Measured by GPC in THF (30 ˚C). [h]Toluene.

The addition of BnOH to initiator **1** proved to be highly beneficial to ROP activity and control (entries 3-5, Table 1), with a 1/1 **1**/BnOH catalytic mixture leading to a 100 fold increase in ROP activity relative to species **1** alone (TOF = 3.8 *vs* 400 h^{-1}; entry 1 *vs* 3, Table 1). In fact, species **1** displays a remarkable ROP activity with the nearly quantitative conversion of 1000 equiv of CL with 15 min at room temperature (TOF = 3720 h^{-1}) to afford narrow disperse and chain-length-controlled PCL (1000/10/1 CL/BnOH/**1**, 93% conv to PCL, M_n = 9900 $g.mol^{-1}$, $Đ$ = 1.06, entry 5, Table 1; Fig. S8, ESI). In contrast, the Ga(II) analogue **2** is significantly less active than its Al counterpart **1** (TOF = 4.2 *vs* 400 h^{-1}; entry 3 *vs* 4, Table 1), in line with the lower Lewis acidity of **2**. For all runs in the presence of BnOH, a good agreement between the expected and experimental chain lengths [M_n(theo) *vs.* M_n(corr)] is observed. For the ROP catalysis with a 1000/3/1 CL/BnOH/**1** ratio (entry 1, Table 2), additional kinetic data were gathered and are all consistent with a well-behaved ROP process, including: i) a first-order dependence on CL concentration after an induction period of

roughly 2 min (Figure 5, k_{obs} = 0.1644 min^{-1}) and ii) a linear correlation between monomer conversion and the M_n values of the produced PCL (Figure S9, ESI). For the PCL produced from a 1000/10/**1** CL/BnOH/1 mixture, MALDI-TOF mass spectrometric data agree with a OBn-end-capped PCL material (Figure S10, ESI).

To our knowledge, such ROP activity at room temperature is unprecedented using Al-based catalysts, species that typically display, at best, moderate cyclic esters ROP activity under such conditions and for which heating is required for high ROP activity.[10] To further optimize the ROP performances of initiator **1**, several additional catalytic runs were done with higher monomer and/or BnOH feeds (Table 2), allowing for instance the ready production of narrow disperse PCL with M_n > 30,000 $g.mol^{-1}$ (entries 1 and 3; Table 2). Regarding ROP activity, at best a 3/1 BnOH/**1** catalytic mixture converted 1330 equiv of CL (67% conv. of 2000 equiv) to PCL within 15 min at room temperature (entry 3, Table 2; TOF = 5320 h^{-1}). A significant decrease in ROP activity occurs however at higher monomer loading (*i.e.* 3000 equiv CL), possibly due to catalyst deactivation by impurities in the monomer source (entries 4 and 5, table 2).

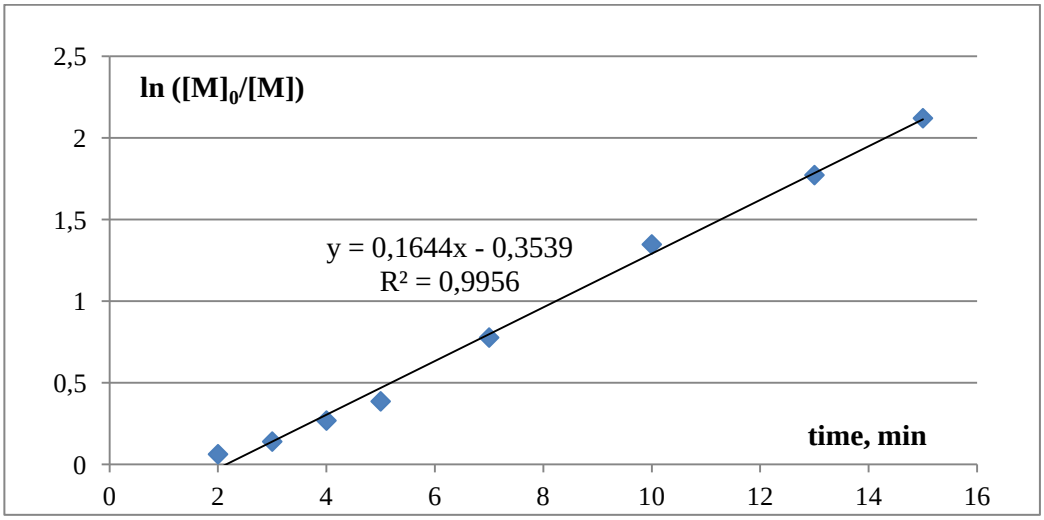

Figure 5. Plot of $ln(M_0/M)$ as a function of the time in the ROP of ε-caprolactone using complex **1** as catalyst (M = CL, conditions: CL/BnOH/**1** in a 1000/3/1 ratio, $[M]_0$ = 1 M, toluene, room temperature).

Table 2. ROP of CL catalyzed by species **1**[a] with various monomer/alcohol feeds

Entry	CL [b]	BnOH [b]	Conversion,%[c]	$M_{n,\,theo}$ [d]	$M_{n,\,corr}$ [e]	$Đ$ [f]	TOF (h^{-1})
1	1000	3	88	33400	37900	1.05	3520
2	1000	5	94	21400	22200	1.13	3760
3	2000	3	67	46400	44700	1.05	5320
4	3000	10	21	7200	6700	1.08	2520
5	3000	30	14	1600	1700	1.11	1680

[a]Polymerization conditions: $[CL]_0$ = 1 M, toluene, room temperature, 15 min. [b] equiv in BnOH *vs* Al initiator. [c] Monomer conversion. [d] Calculated using $M_{n,theo} = [CL]_0/[BnOH]_0 \times M_{CL} \times$ conv. [e] Measured by GPC in THF (30 ˚C) using PS standards and corrected by applying the appropriate correcting factor (0.56). [f]Measured by GPC in THF (30 ˚C).

The presence of an induction period in the ROP of CL initiated by **1**/BnOH (roughly 2 min in Figure 5) suggests that the formation of the active ROP catalyst requires a prior reaction of **1** with BnOH. The reaction of the Al(II) species **1** with BnOH (1 or 2 equiv) was thus NMR monitored (- 40 °C and room temperature), yet only evidencing the alcoholysis of species **1** by BnOH to protio-ligand dpp-bianH_2 and unidentified organoaluminum species.

Compounds **1** and **2** were also found to initiate the ROP of TMC in the presence/absence of BnOH at room temperature, but, in the case of **1**, with a lower catalytic activity than that observed with CL (Table S2, ESI). As seen with CL, the ROP of TMC is rather uncontrolled in the absence of BnOH with the production of PTMC with much larger M_n values than theoretically expected. The addition of BnOH allows the production of chain-length controlled PTMC with a narrow polydispersity (entry 2, table S2).

ROP of CL mediated by 1/BnOH: a DFT-estimated mechanism. The lack of experimental data rationalizing the high CL ROP activity of dinuclear Al(II) species **1** in the presence of BnOH prompted us toward DFT computational studies for mechanistic

understanding. All calculations were all performed at the B3LYP/6-31+G** or B3LYP/def2-SVP theory level. For reasonable calculations time, the N-*dpp* substituents were replaced by N-*Me* group in all calculated models. The results of these calculations were then validated with N-*dpp* bian models for a reaction step (*vide infra* and Figures S19–S23, ESI).

The overall mechanism for the ROP of CL by **1**/BnOH is depicted in Figure 6. Under CL ROP conditions (thus in the presence of a large excess of CL and a few equiv of BnOH *vs.* **1**), the *bis*-CL model adduct **B** (ΔG = -12.0 kcal.mol^{-1}, Figure 6; Figure S11, ESI) readily forms upon coordination of 2 equiv of CL to **A**, a reaction thermodynamically favored. Adduct **B** then reacts with 1 equiv of BnOH to afford the BnOH-Al–Al-CL adduct **C** (ΔG = -12.6 kcal.mol^{-1}; Figure S12, ESI), which undergoes an intramolecular proton transfer to a nitrogen of the (bian)Al moiety to afford the Al(II)-OBn complex **D** (ΔG = -33.3 kcal.mol^{-1}, Figure S14, ESI). Proton transfer leading to **D** from **C** then occurs through transition state [**C-D**]‡ (ΔG = -5.3 kcal.mol^{-1}, Figure S13, ESI) with a low barrier process ($\Delta\Delta G$ = 7.3 kcal.mol^{-1}). The reaction is also clearly thermodynamically driven by the stability of **D**. Such alcoholysis reaction is also in line with the typical reactivity of dpp-bian main group metal complexes with protic substrates.[11] Thus, **D** is a realistic model intermediate forming upon from a **1**/BnOH mixture under CL ROP conditions. Intermediate **D** then undergoes an intramolecular nucleophilic attack of the Al(II)–*OBn* group to the CL moiety to yield metallacycle **E** *via* transition state [**D-E**]‡ (ΔG = -6.2 kcal.mol^{-1}, Figure 6; Figure S15, ESI). The energy barrier for the formation of **E** from **D** ($\Delta\Delta G$ = 27.1 kcal.mol^{-1}) is the largest of the all computed ROP mechanism, in line with such a step being rate-determining. Model **E** (ΔG = -13.9 kcal.mol^{-1}; Figure 6; Figure S16, ESI) is unstable and ring-opens through a nearly barrierless step *via* transition state [**E-F**]‡ (ΔG = -13.0 kcal.mol^{-1}, barrier: $\Delta\Delta G$ = 0.9 kcal.mol^{-1}; Figure S17, ESI) to yield the thermodynamically more stable and ring-opened product **F** (ΔG = -33.3 kcal.mol^{-1}; Figure 6; Figure S18, ESI).

In addition to the above calculations (computed with smaller N-*Me* substituents), the ROP mechanism with the larger N-*dpp* substituents (as those in species **1**) was partially computed up to the formation of a model of type **D**: it led to similar energy barriers to those for the less bulky N-*Me* systems (see models **B'**, **C'**, **[C'-D']**‡ and **D'** and associated mechanism; Figures S19–S23, ESI). It should also be mentioned that an alternative pathway was considered and DFT computed starting from the Al–BnOH adduct **C**: *i.e.* an intramolecular oxidative addition of BnOH to the Al(II)–Al(II) bond of **C** to afford models (Me-bian)Al–H and (Me-bian)Al(OBn)(CL). However, besides being unlikely on the basis of experimental observations, the overall ROP mechanism is also endergonic (by 12 kcal.mol^{-1}), ruling out such an option.

Based on DFT data, the most reasonable ROP mechanism for CL polymerization by **1**/BnOH thus suggests co-operation of the proximal Al(II) centers: this is clearly evidenced by the structures of model intermediates/products **D**, **E** and **F** and associated transtion states. Such cooperative effects provide a rationale to the high ROP activity observed for (Me-bian)Al–Al(Me-bian) system **1**. The observation of an induction period in the ROP of CL by **1**/BnOH may also be explained in view of the proposed mechanism: *i.e.* the required time for the formation of the Al–OBn species (model **D**) from *bis*-CL adduct **C** and BnOH.

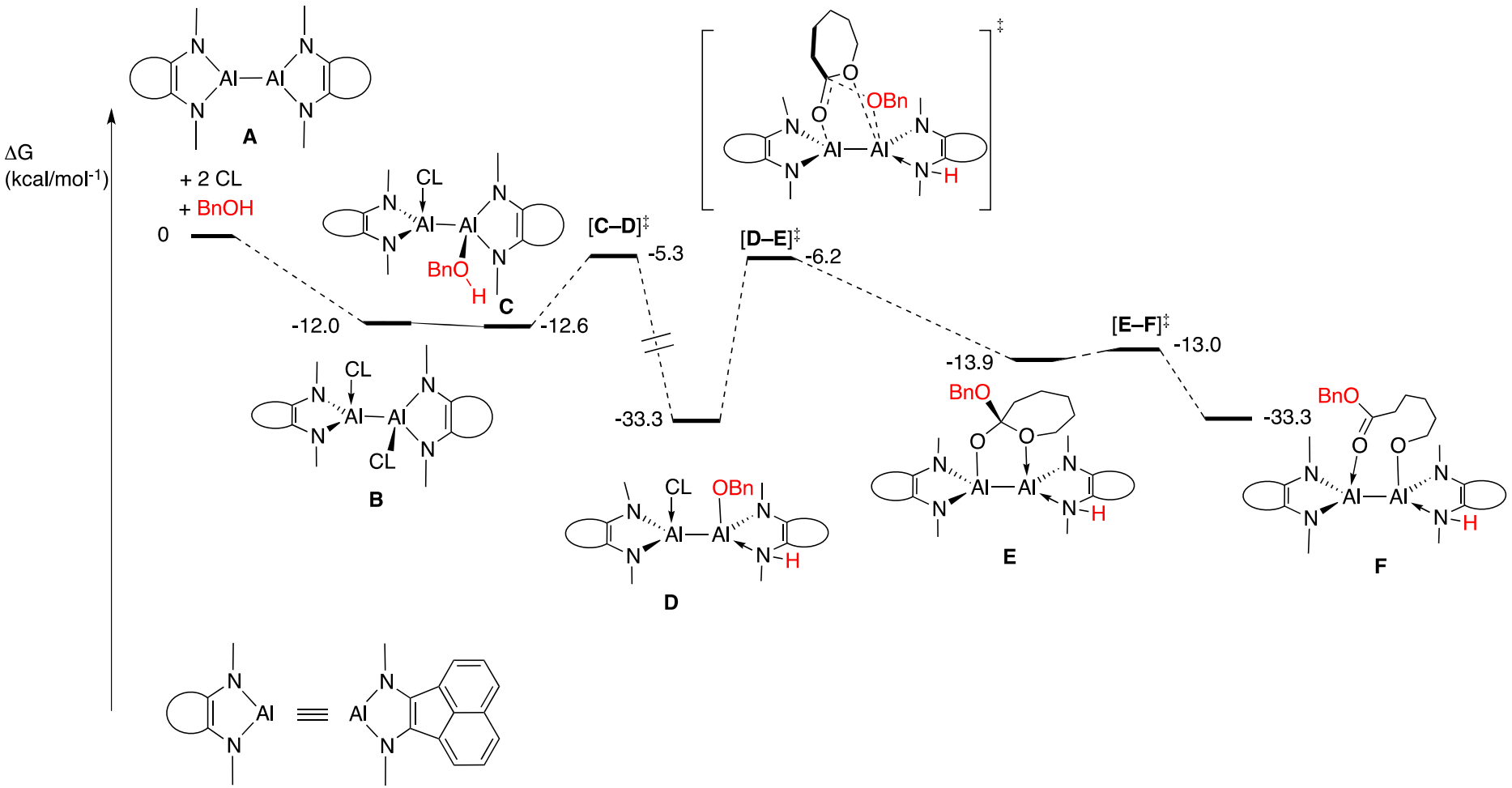

Figure 6. DFT-estimated (B3LYP/6-31+G** theory level) Gibbs free energy profile for the mechanism of CL ROP mediated by **A**/BnOH

ROP of CL by Al(III) alkoxide species (dpp-bian)Al(κ^2-{$OCH_2CH_2NMe_2$}) (5). For comparison with the Al(II) species **1,** the higher oxidation state Al(III) analogue (dpp-bian)Al(κ^2-{$OCH_2CH_2NMe_2$}) (**5**) was also prepared and characterized for use in the ROP of CL. Species **5** was synthesized by reaction of (dpp-bian)AlCl(Et_2O), generated *in situ* according to a reported procedure,[12] with 1 equiv of [$OCH_2CH_2NMe_2$]Na (Et_2O, room temperature; Scheme 2). Compound **5** was isolated as deep blue X-ray quality crystals and its molecular structure was determined by XRD analysis (Figure 7), confirming the expected formulation deduced from NMR and combustion analysis data.

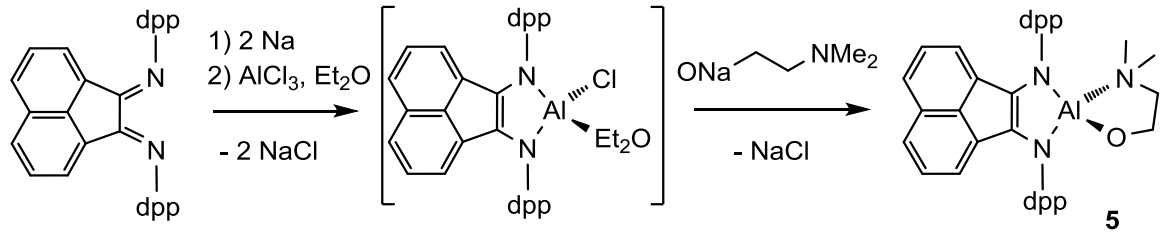

Scheme 2. Synthesis of the dpp-bian-supported Al(III)-alkoxide **5**

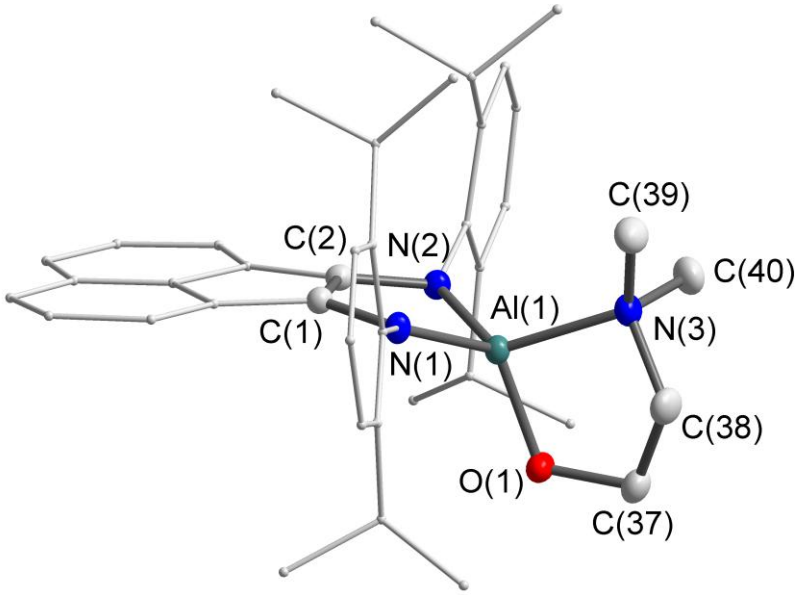

Figure 7. Molecular structure of species **5**. Thermal ellipsoids are at 50% probability. Hydrogen atoms are omitted. Selected bond lengths (Å) and angles (°): Al(1)–N(3) 1.9722(15), C(1)–C(2) 1.380(2), C(1)–N(1) 1.402(2), C(2)–N(2) 1.408(2), Al(1)–N(1)

1.8381(14), Al(1)–N(2) 1.8332(14), Al(1)–O(1) 1.7411(13), O(1)–C(37) 1.414(2), N(2)–Al(1)–N(3) 120.73(6), N(1)–Al(1)–O(1) 121.03(7), O(1)–Al(1)–N(3) 90.24(6), N(1)–Al(1)–N(2) 94.08(6).

As depicted in Figure 7, species **3** features a central four-coordinate Al(III) center in a tetrahedral geometry and effectively chelated in a bidentate κ^2-fashion by the di-anionic $[dpp\text{-}bian]^{2-}$ ligand and the amino-alkoxide moiety $[OCH_2CH_2NMe_2]^-$. Geometrical and bonding parameters are normal for complex **3**, and it is structurally similar to its gallium analogue (dpp-bian)Ga(κ^2-{$OCH_2CH_2NMe_2$}) earlier reported.[13] Unlike dinuclear Al(II) species **1**, the Al(III) species **5** is only poorly active in the ROP of CL at room temperature with a 15% conv. to PTMC (1000 equiv of TMC, 10/1 BnOH/**5** catalyst mixture) within 24h at room temperature, thus contrasting the higher ROP performance of BnOH/**1** under identical conditions (TOF = 3720 *vs.* 6.25 h^{-1}).

Conclusion

The reactivity of dinuclear low valent Al(II) and Ga(II) complexes of the type (dpp-bian)M–M(dpp-bian) (M = Al, Ga) towards CL and TMC was first investigated. While CL and TMC both readily coordinates to the Al(II) species **1** to form the corresponding *bis*-adducts **3** and **4**, the less Lewis acidic Ga(II) analogue **2** is unreactive with such polar substrates at room temperature. Though stable on their own, *bis*-adducts **3** and **4** readily initiate at room temperature the ROP of CL and TMC under catalytic conditions in the presence of BnOH. In the case of CL, the ROP activity of species **1** in the ROP of CL at room temperature is remarkable since outperforming all its Al(III) congeners thus far reported under such conditions. Detailed DFT studies on the CL ROP mediated by initiator **1**/BnOH agree with a mechanism involving a co-operation between the two Al(II) metal centers (in **1**)

for the ring-opening of CL to proceed. Such bimetallic co-operativity occurs thanks to the two directly bonded and thus very proximal Al(II) centers, which is proposed to account for the observed ROP performance of species **1**.

Experimental section

General remarks. Air sensitive experiments were carried out under vacuum using standard Schlenk line techniques or in a nitrogen-filled MBraun Unilab glovebox. Dichloromethane, pentane, toluene and diethyl ether were first dried through a solvent purification system (MBraun SPS) and stored for at least 48 h over activated molecular sieves (4 Å) in a glovebox prior to use. Tetrahydrofuran was distilled over Na/benzophenone and stored over activated molecular sieves (4 Å) for a 48 h in a glovebox prior to use. Methanol and benzyl alcohol were distilled over KOH and stored over activated molecular sieves (4 Å) for a couple of days in a glovebox prior to use. Trimethylene carbonate (TMC) was purchased from either T.C.I. Europe Corporation or Boehringer: it was dried over CaH_2 in THF for 24 h and precipitated with pentane prior to use. ε-Caprolactone (CL) was purchased from Aldrich, distilled over CaH_2 and stored over molecular sieves for at least 24 h in the glovebox prior to use. All other chemicals were purchased from Aldrich and were used as received. The NMR spectra were recorded on Bruker AC 300 and 400 MHz NMR spectrometers. For air and moisture sensitive experiments were carried out in Teflon-valved J. Young NMR tubes at ambient temperature. ^{1}H and ^{13}C chemical shifts are reported *vs* $SiMe_4$ and were determined by reference to the residual ^{1}H and ^{13}C solvent peaks. Elemental analyses for compounds were performed at the Service of Microanalysis of the Minin University (Nizhny Novgorod, Russia). The IR spectra were recorded on the FSM-1201 spectrometer in a Nujol mull. GPC analyses were performed on a system equipped with a Shimadzu RID10A refractometer detector using HPLC-grade THF as an eluant. Molecular weights and polydispersity indices ($Đ$) were calculated using polystyrene standards. In the case of molecular weight number (M_n), these were corrected with appropriate correcting factors for PCL and PTMC.[14,15] MALDI-TOF mass spectroscopic analyses were performed at the Service de Spectrométrie de Masse de l'Institut de Chimie de Strasbourg and run in a positive mode: samples were prepared by

mixing a solution of the polymers in CH_2Cl_2 with a 0.5 mg/100 mL concentration, and 2,5-dihydroxybenzoic acid (DHB) was used as the matrix in a 5/1 volume ratio. Crystal data were collected at 173 K using Mo (for **3** and **5**) or Cu (for **4**) Kα graphite-monochromated (λ = 0.71073 and 1.54178 Å consequently) radiation on a Bruker APEX-II CCD diffractometer. The structures were solved using direct methods with SHELXL-2013. Non-hydrogen atoms were refined anisotropically. Hydrogen atoms were generated according to stereochemistry and refined using a riding model in SHELXL-2014/7 (for species **3**) and SHELXL-2013 (for species **5**). Compounds **1** and **2** were prepared according to literature procedures.[16]

Computational Investigation. All calculations were performed using Gaussian 09 package (version D01) at the DFT level of theory (B3LYP functional) with Pople's 6-31+G** basis set on all atoms. Solvent corrections (toluene) were included through a PCM model. Dispersion corrections were taken into accounts through Grimme's corrections. All energies are Free enthalpies in kcal.mol^{-1}. Full geometry optimizations were performed on all complexes. Minima were characterized by a full set of real frequencies and transitions states by one and only one imaginary frequency. The minima connected by a TS were identified through an intrinsic reaction coordinate procedure. To reduce the computational cost the structure of the complex was simplified as shown in Figure 6. Due to computational cost, the calculations on the complete structure in ESI were done with a smaller basis set, namely the def2-SVP.

(dpp-bian)($C_4H_6O_3$)Al–Al($C_4H_6O_3$)(dpp-bian) (3)

In glovebox 10 ml toluene solution of compound (dpp-bian)Al-Al(dpp-bian) (**1**) (40 mg, 0.035 mmol) were mixed with 5 ml toluene solution of TMC (7.1 mg, 0.07 mmol) at room temperature. The reaction mixture turned from deep-violet to green immediately. Deep green square crystals of **3** were formed after 24 hours at –35 °C. Yield 22.4 mg (51%). ^{1}H NMR 300

MHz, C_6D_6, ppm): δ 7.35-7.24 (m, 6 H_{arom}), 7.01 (d, 2 H_{arom}, 8.0 Hz), 6.83 (dd, 2 H_{arom}, 6.8 and 8.2 Hz), 6.00 (d, 2 H_{arom}, 6.8 Hz), 3.73 (s, 4 H C*H*$(CH_3)_2$, 6.6 Hz), 3.03 (m, 4 H, TMC), 1.15 (d, 12 H, CH(C*H*$_3$)(CH_3) 6.8 Hz), 1.09 (broad d, 12 H, CH(CH_3)(C*H*$_3$), 6.6 Hz), 0.47 (quint, 2 H TMC, 5.9 Hz). The low solubility of the *bis*-TMC adduct **3** precluded the obtainment of exploitable ^{13}C NMR data. IR (Nujol, ν, cm^{-1}): 464.6 m, 496.6 s, 518.2 m, 548.8 w, 571.0 m, 627.3 m, 650.8 m, 681.2 s, 694.7 w, 727.5 vs, 743.0 w, 758.4 m, 768.0 w, 800.0 s, 813.9 m, 835.3 w, 919.3 s, 936.4 m, 956.2 w, 962.2 w, 1031.0 w, 1040.2 w, 1058.2 w, 1122.2 m, 1158.6 s, 1178.2 w, 1191.1 w, 1253.5 m, 1270.9 w, 1456 vs, 1511.1 m, 1544.7 s, 1625 s, 1746 vs, 2334.7 w, 3060.1 w. Calculated for $C_{80}H_{92}Al_2N_4O_6$: C, 76.28; H, 7.36; N, 4.45; O, 7.62. Found: C, 76.46; H, 7.38.

(dpp-bian)($C_6H_{10}O_2$)Al–Al($C_6H_{10}O_2$)(dpp-bian) (4)

In glovebox 10 ml toluene solution of compound (dpp-bian)Al-Al(dpp-bian) (**1**) (40 mg, 0.035 mmol) were mixed with 5 ml toluene solution of ε-caprolactone (8 mg, 0.07 mmol) at room temperature. The reaction mixture turned from deep-violet to green immediately. Deep green square crystals of **4** (as a toluene solvate) formed after 24 h at –35 °C. Yield 25.0 mg (52 %). ^{1}H NMR (500 MHz, C_6D_6, ppm) δ 7.31-7.22 (m, 6 H_{arom}), 7.01 (d, 2 H_{arom}, 8.2 Hz), 6.83 (dd, 2 H_{arom}, 7.3 and 8.2 Hz), 6.02 (d, 2 H_{arom}, 6.7 Hz), 3.73 (br s, 4 H C*H*$(CH_3)_2$, 6.4 Hz), 3.11 (br t, 2 H, OC*H*$_2$, CL), 1.95 (br t, 2 H, C(O)C*H*$_2$, CL), 1.14 (d, 12 H, CH(C*H*$_3$)(CH_3) 6.7 Hz), 1.04 (broad d, 12 H, CH(CH_3)(C*H*$_3$), 6.4 Hz), 0.96 (br q, 2 H, CL), 0.82-0.70 (br m, 4 H, CL). ^{13}C NMR (125 MHz, C_6D_6, ppm): 21.45 (*C*H_3, toluene), 21.93 (*C*H_2 CL), 25.17 (*C*H_3 iPr), 25.54 (*C*H_3 iPr), 27.33 (*C*H_2 CL), 28.07 (*C*H_2 CL), 28.48 (*C*H_3 iPr), 34.45 (*C*H_2 CL), 73.49 (O*C*H_2 CL), 117.69 (*C*H napht), 123.45 (*C*H Ar), 123.67 (*C*H Ar), 125.02 (*C*H napht), 127.11(*C* napht), 127.23 (*C*H napht), 127.53 (*C* napht), 128.50 (*C* napht), 135.55 (C=O CL), 136.40 (*C*-N bian), 144.50(C_{ipso}), 146.53 (*C*-iPr). IR (Nujol, ν, cm^{-1}): 454.6 w, 464.4 m, 520.2 w 544.3 vw, 578.4 w, 623.6 w, 648.4 w, 669.0 vw, 694.7 m, 761.1 vs, 781.4 w, 801.9 m,

809.9 m, 817.3 w, 834.6 vw, 849.6 w, 859.6 w, 890.4 m, 917.9 s, 935.9 m, 961.6 w, 986.8 vw, 999.3 vw, 1015.0 w, 1042.0 s, 1057.4 m, 1100.4 m, 1134.0 w, 1164.8 s, 1178.7 s, 1190.1 m, 1206.6 w, 1252.0 s, 1311.7 s, 1324.7 m, 1458.4 vs, 1494.6 w, 1513.4 s, 1542.4 m, 1589.2 m, 1615.1 s, 1666.1 w, 1732.5 vs, 1851.2 vw, 1910.8 w, 3380.4 w, 3058.1 w, 3622.5 3688.1 vw. Calculated for $C_{91}H_{108}Al_2N_4O_4$: C, 79.44; H, 7.91; O, 4.65. Found: C, 79.52; H, 7.99.

(dpp-bian)Al(κ^2-{$OCH_2CH_2NMe_2$}) (5)

In glovebox to 30 ml diethyl ether solution of (dpp-bian)AlCl(Et_2O) (prepared *in situ* from 500 mg (1 mmol) of dpp-bian ligand) and sodium alkoxide $NaOCH_2CH_2NMe_2$ (110 mg, 1 mmol) was added at room temperature. The reaction mixture was stirred for 10 minutes, during which time a slight color change from blue-violet to blue was observed. The reaction mixture was filtered (filter pore 4) and then concentrated to 20 ml. Deep blue square crystals of **5** was obtained at room temperature within 18 h. Yield 130 mg (21 %, crystals). ^{1}H NMR (500 MHz, C_6D_6, ppm): 7.32–7.27 (m, 4 H_{arom}), 7.23 (dd, 2 H_{arom}, 7.0 and 2.4 Hz), 7.10 (d, 2 H_{arom}, 8.2Hz), 6.86 (dd, 2 H_{arom}, 7.0 and 8.2 Hz), 6.19 (d, 2 H_{arom}, 6.9 Hz), 4.27 (sept, 2 H C*H*$(CH_3)_2$, 6.9 Hz), 3.76 (sept, 2 H C*H*$(CH_3)_2$, 6.9 Hz), 3.49 (t, 2 H, OC*H*$_2$, 5.6 Hz), 1.71 (t, 2 H, N-C*H*$_2$, 5.6 Hz), 1.70 (s, 6 H, N(C*H*$_3)_2$, 1.41 (d, 6 H, CH(C*H*$_3)_2$, 6.9 Hz), 1.20 (d, 6 H, 6.9 Hz), 1.19 (d, 6 H, 6.9 Hz), 1.17 (d, 6 H, 6.9 Hz). ^{13}C NMR (125 MHz, C_6D_6, ppm): 24.70 (*C*H_3 iPr), 25.21 (*C*H_3 iPr), 25.40 (*C*H_3 iPr), 25.60 (*C*H_3 iPr), 28.39 (*C*H iPr), 28.43 (*C*H iPr), 43.97 (N(*C*$H_3)_2$), 57.55 (OCH_2), 63.24 (N*C*H_2), 118.23 (*C*H napht), 123.94 (*C*H napht), 124.10 (*C*H Ar), 124.25 (*C*H Ar), 125.45 (*C*H Ar), 127.24 (*C*H napht), 127.39 (C napht), 127.46 (C napht), 132.21 (C napht), 136.58 (*C*-N bian), 143.50 (C_{ipso}), 146.61 (*C*-iPr), 146.81 (*C*-iPr).

ROP of CL and TMC by species 3-5

In a glovebox, the initiator **3-5** was charged in a vial equipped with a Teflon™-tight screw-cap, a monomer (M = TMC or CL) solution and a BnOH solution (so that $[M]_0$ = 1 M in toluene) was added *via* a syringe all at once. The resulting solution was vigorously stirred for the appropriate time at room temperature. When the desired time was reached, aliquots were taken and analyzed by ^{1}H NMR spectroscopy to estimate the conversion to PCL or PTMC. The reaction mixture was exposed to air and volatiles removed under vacuum; the resulting solid was then washed several times with MeOH, dried in vacuo until constant weight and subsequently analyzed by ^{1}H NMR and SEC.

Conflicts of interest

There are no conflicts to declare.

Acknowledgments. The authors thank the CNRS and the University of Strasbourg for financial support. O. K. is grateful to the French Embassy in Russia (Moscow, Russia) for a Mechnikov Fellowship. We acknowledge the Russian Scientific Foundation (grant 17-73-20356) for financial support on the synthesis and spectroscopic investigation of metal complexes.

Supporting Information. NMR data, selected GPC and polymerization kinetics data. DFT calculations details and structures of all computed models (xyz file). The crystallographic information files (CIF) of **3**, **4**-toluene and **5** have been deposited to the CCDC, 12 Union Road, Cambridge, CB2 1EZ, U.K., and can be obtained on request free of charge, by quoting the publication citation and deposition numbers 1851716-185718. See DOI: 10.1039/x0xx00000x.

References

1. (a) M. Labet, W. Thielemans, *Chem. Soc. Rev.*, 2009, **38**, 3484; (b) M. A. Woodruff, D. W. Hutmacher, *Prog. Polym. Sci.*, 2010, **35**, 1217.

2 . (a) A. Y. Yuen, E. Lopez-Martinez, E. Gomez-Bengoa, A. L. Cortajarena, R. H. Aguirresarobe, A. Bossion, D. Mecerreyes, J. L. Hedrick, Y. Y. Yang and H. Sardon, *ACS Biomater. Sci. Eng.*, 2017, **3**, 1567; (b) S. Tempelaar, L. Mespouille, P. Dubois and A. P. Dove, *Macromolecules*, 2011, **44**, 2084 ; (c) T. Artham and M. Doble, *Macromol. Biosci.*, 2008, **8**, 14.

3. Selected reviews on metal-based ROP of CL (a) A. Arbaoui, C. Redshaw, *Polym. Chem.*, 2010, **1**, 801, (b) B. J. O'Keefe, M. A. Hillmeyer, W. B. Tolman, *J. Chem. Soc., Dalton Trans*., 2001, 2215.

4. Selected recent examples on metal-mediated ROP of TMC: (a) M. Helou, O. Miserque, J.-M Brusson, S. M. Guillaume, J.-F. Carpentier, *ChemCatChem*, 2010, **2**, 306; (b) J. Koller, R. G. Bergman, *Organometallics*, 2011, **30**, 3217; (c) F. Hild, L. Brelot, S. Dagorne, *Organometallics*, 2011, **30**, 5457; (d) F. Hild, N. Neehaul, F. Bier, M. Wirsum, C. Gourlaouen, S. Dagorne, *Organometallics*, 2013, **32**, 587; (e) C. Fliedel, S. Mameri, S. Dagorne, T. Avilés, *Appl. Organomet. Chem.*, 2014, **28**, 504.

5. (a) M. Normand, T. Roisnel, J.-F. Carpentier, E . Kirillov, *Chem. Commun.*, 2013, **49**, 11692; (b) Y. Ma, H. Ma, *Chem. Commun.*, 2012, **48**, 6729; (c) F. Isnard, M. Lamberti, L. Lettieri, I. D'auria, K. Press, R. Troiano, M. Mazzeo, *Dalton Trans.*, 2016, **45**, 16001; (d) L. Chen, W. Li, D. Yuan, Q. Shen, Y. Yao, *Inorg. Chem.*, 2015, **54**, 4699; (e) A. Thévenon, C. Romain, M. S. Bennington, A. J. P. White, H. J. Davidson, S. Brooker, C. K. Williams, *Angew. Chem. Int. Ed.*, 2016, **55**, 8680.

6. (a) K. M. Osten, P. Mehrkhodavandi, *Acc. Chem. Res.*, 2017, **50**, 2861; (b) A. Pietrangelo, S. C. Knight, A. K. Gupta, L. J. Yao, M. A. Hillmeyer, W. B. Tolman, *J. Am. Chem. Soc.*, 2010, **132**, 11649; (c) I. Yu, A. Acosta-Ramirez, P. Mehrkhodavandi, *J. Am. Chem. Soc.*,

2012, **134**, 12758; (d) J. Fang, I. Yu, P. Mehrkhodavandi, L. Maron, *Organometallics*, 2013, **32**, 6950; (e) C. Fliedel, D. Vila-Viçosa, M. J. Calhorda, S. Dagorne, T. Avilés, *ChemCatChem*, 2014, **6**, 1357; (f) S. R. Kosuru, T.-H. Sun, L.-F. Wang, J. K. Vandavasi, W.-Y. Lu, Y.-C. Lai, S. C. N. Hsu, M. Y. Chiang, H.-Y. Chen, *Inorg. Chem.*, 2017, **56**, 7998; (g) A. B. Kremer, R. J. Andrews, M. J. Milner, X. R. Zhang, T. Ebrahimi, B. O. Patrick, P. L. Diaconescu, P. Mehrkhodavandi, *Inorg. Chem.*, 2017, **56**, 1375.

7. (a) I. L. Fedushkin, A. S. Nikipelov, A. A. Skatova, O. V. Maslova, A. N. Lukoyanov, G. K. Fukin, A. V. Cherkasov, *Eur. J. Inorg. Chem.*, 2009, 3742; (b) I. L. Fedushkin, A. N. Lukoyanov, A. N. Tishkina, G. K. Fukin, K. A. Lyssenko, M. Hummert, *Chem. Eur. J.*, 2010, **16**, 7563; (c) I. L. Fedushkin, A. S. Nikipelov, K. A. Lyssenko, *J. Am. Chem. Soc.*, 2010, **132**, 7874; (d) I. L. Fedushkin, M. V. Moskalev, A. N. Lukoyanov, A. N. Tishkina, E. V. Baranov, G. A. Abakumov, *Chem. Eur. J.*, 2012, **18**, 11264; (e) I. L. Fedushkin, A. S. Nikipelov, A. G. Morozov, A. A. Skatova, A. V. Cherkasov, G. A. Abakumov, *Chem. Eur. J.*, 2012, **18**, 255; (f) T. Sanden, M. T. Gamer, A. A. Fagin, V. A. Chudakova, S. N. Konchenko, I. L. Fedushkin, P. W. Roesky, *Organometallics*, 2012, **31**, 4331; (g) I. L. Fedushkin, M. V. Moskalev, A. A. Skatova, G. K. Fukin, G. A. Abakumov, *Russ. Chem. Bull.*, 2013, **62**, 731; (h) I. L. Fedushkin, A. A. Skatova, V. A. Dodonov, V. A. Chudakova, N. L. Bazyakina, A. V. Piskunov, S. V. Demeshko, G. K. Fukin, *Inorg. Chem.*, 2014, **53**, 5159; (i) I. L. Fedushkin, V. G. Sokolov, A. V. Piskunov, V. M. Makarov, E. V. Baranov, G. A. Abakumov, *Chem. Comm.*, 2014, **50**, 10108; (j) O. V. Kazarina, M. V. Moskalev, I. L. Fedushkin, *Russ. Chem. Bull.*, 2015, **64**, 32; (k) M. V. Moskalev, A. A. Skatova, V. A. Chudakova, N. M. Khvoinova, N. L. Bazyakina, A. G. Morozov, O. V. Kazarina, A. V. Cherkasov, G. A. Abakumov, I. L. Fedushkin, *Russ. Chem. Bull.*, 2015, **64**, 2830; (l) M. V. Moskalev, A. M. Yakub, A. G. Morozov, E. V. Baranov, O. V. Kazarina, I. L. Fedushkin, *Eur. J. Org. Chem.*, 2015, 5781; (m) I. L. Fedushkin, A. A. Skatova, V. A. Dodonov, X. J. Yang, V. A. Chudakova, A. V. Piskunov, S. Demeshko, E. V. Baranov, *Inorg. Chem.*, 2016, **55**, 9047; (n) I. L. Fedushkin, V. A. Dodonov, A. A. Skatova, V. G. Sokolov, A. V. Piskunov, G. K. Fukin, *Chem. Eur. J.*, 2018, **24**, 1877.

8. S. Dagorne, C. Fliedel, *Top. Organomet. Chem.*, 2013, **41**, 125; (b) S. Dagorne, M. Normand, E. Kirillov, J.-F. Carpentier, *Coord. Chem. Rev.*, 2013, **257**, 1869.

9. (a) S. Dagorne, F. Le Bideau, R. Welter, S. Bellemin-Laponnaz, A. Maisse-François, *Chem. Eur. J.*, 2007, **13**, 3202; (b) J. Lewiński, P. Horeglad, E. Tratkiewicz, W. Grzenda, J. Lipkowski,E. Kolodziejczyk, *Macromol. Rapid Commun.*, 2004, **25**, 1939.

10. For examples of Al-based catalysts exhibiting CL ROP activity at room temperature, see, for instance: (a) F. Hild, N. Neehaul, F. Bier, M. Wirsum, C. Gourlaouen, S. Dagorne, *Organometallics*, 2013, **32**, 587; (b) A. Amgoune, L. Lavanant, C. M. Thomas, Y. Chi, R. Welter, S. Dagorne, J.-F. Carpentier, *Organometallics*, 2005, **24**, 6279.

11. (a) I. L. Fedushkin, N. M. Khvoinova, A. A. Skatova, G. K. Fukin, *Angew. Chem. Int. Ed. Engl.*, 2003, **42**, 5223; (b) I. L. Fedushkin, V. A. Chudakova, G. K. Fukin, S. Dechert, M. Hummert, H. Schumann, *Russ. Chem. Bull.*, 2004, **53**, 2744; (c) I. L. Fedushkin, A. G. Morozov, O. V. Rassadin, G. K. Fukin, *Chem. Eur. J.*, 2005, **11**, 5749; (d) I. L. Fedushkin, A. A. Skatova, G. K. Fukin, M. Hummert, H. Schumann, *Eur. J. Inorg. Chem.*, 2005, 2332; (e) I. L. Fedushkin, V. A. Chudakova, M. Hummert, H. Schumann, *Z. Naturforsch. B Chem. Sci.*, 2008, **63**, 161.

12. I. L. Fedushkin, A. N. Lukoyanov, G. K. Fukin, M. Hummert, H. Schumann, *Russ. Chem. Bull.*, 2006, **55**, 1177.

13. I. L. Fedushkin, O. V. Kazarina, A. N. Lukoyanov, A. A. Skatova, N. L. Bazyakina, A. V. Cherkasov, E. Palamidis, *Organometallics*, 2015, **34**, 1498.

14. M. Save, M. Schappacher, A. Soum, *Macromol. Chem. Phys*., 2002, **203**, 889.

15. D. Delcroix, B. Martin-Vaca, D. Bourissou, C. Navarro, *Macromolecules*, 2010, **43**, 8828.

16. (a) I. L. Fedushkin, M. V. Moskalev, A. N. Lukoyanov, A. N. Tishkina, E. V. Baranov, G. A. Abakumov, *Chem. Eur. J.*, 2012, **18**, 11264 ; (b) I. L. Fedushkin, A. N. Lukoyanov, S. Y. Ketkov, M. Hummert, H. Schumann, *Chem. Eur. J.*, 2007, **13**, 7050.